

## The orthoenstatite liquidus field in the system forsterite–diopside–silica at one atmosphere

JOHN LONGHI AND ALAN E. BOUDREAU

*Department of Geology, University of Oregon  
Eugene, Oregon 97403*

### Abstract

Melting experiments at one atmosphere show a liquidus field of orthoenstatite in the system forsterite–diopside–silica. The orthoenstatite liquidus field is intermediate in CaO content between the protoenstatite and pigeonite fields and intermediate in SiO<sub>2</sub> content between the forsterite and tridymite fields. Previously unrecognized peritectic points are Fo + Pr + OEn + L (1445±5°C), Fo + OEn + Pi + L (1410±5°C), Trid + Pr + OEn + L (1419±5°C), and Trid + OEn + Pi + L (1387±5°C). Orthoenstatite (6–9 wt. percent diopside) is intermediate in composition between protoenstatite (<3 wt. percent diopside) and pigeonite (12–25 wt. percent) in the melting interval. In the subsolidus region there are two distinct fields of orthoenstatite separated by a 275°C interval. With addition of Al to the system or with an increase of 2 kbar pressure the orthoenstatite fields apparently expand and become continuous.

### Introduction

The system forsterite–diopside–silica is one of the classic ternary systems in igneous petrology. Within its boundaries liquidus relations are quite varied—a thermal divide, incongruent melting, several peritectics, and liquid immiscibility (Bowen, 1914; Kushiro, 1972)—and have served several generations of petrologists as useful, but simplified, analogues for olivine/pyroxene crystallization relationships in basaltic magmas.

Less certain are the details of pyroxene phase relations and solid solutions that have challenged numerous investigators (Atlas, 1952; Boyd and Schairer, 1964; Yang and Foster, 1972; Yang, 1973; Warner, 1975). For more than half a century only one low-Ca pyroxene was recognized—protoenstatite—that inverts to clinoenstatite upon quenching, producing cracks and polysynthetic twinning (*e.g.* Smith, 1969). Boyd and Schairer (1964) presented evidence from X-ray diffraction studies suggesting a second low-Ca pyroxene. This evidence was confirmed by Warner (1971), Yang and Foster (1972), and Kushiro (1972) who identified a low-Ca clinopyroxene, “iron-free pigeonite,” with the aid of X-ray and electron microprobe analysis. Studies by Kushiro and Yang attempted to pin down the temperature–composition relationships of the pyroxene phases. Both studies produced phase diagrams of the enstatite–diopside

join with similar topologies (Kushiro, 1972, Fig. 2; Yang, 1973, Fig. 1): protoenstatite is the liquidus pyroxene at high temperature along the enstatite end of the join; at a temperature between 1420° and 1445°C both authors show a reaction between protoenstatite and liquid to form pigeonite, though they differ on the exact temperature; at the pseudo-eutectic (actually a ternary peritectic) forsterite, pigeonite, and diopside coexist with liquid; in the subsolidus region the pigeonite field shrinks with decreasing temperature as the protoenstatite + pigeonite and pigeonite + diopside two-phase fields expand. Yang determined the compositional range of analogous solvi and reversed the reaction pigeonite  $\rightleftharpoons$  orthorhombic pyroxene + diopside at 1276°C in the system forsterite–diopside–silica–anorthite; he then projected these relations onto the enstatite–diopside join.

Recently, Longhi (1978) reported two coexisting low-Ca pyroxenes in the system forsterite–diopside–silica–anorthite at temperatures from 1267° to ~1200°C. These were initially called “orthopyroxene” and “pigeonite,” but re-examination has shown both phases to be orthorhombic pyroxenes: the one poorer in Ca has cracks and polysynthetic twinning usually attributed to protoenstatite inverted to clinoenstatite; the other, richer in Ca, is free of cracks or twinning. Careful scrutiny of the Kushiro and Yang papers reveals several discrepancies, *e.g.* the

protoenstatite solvi in the two phase diagrams do not coincide and Kushiro's protoenstatite has cracks whereas Yang's "protoenstatite" does not. The various observations and discrepancies may be resolved by the recognition of a third low-Ca pyroxene free of cracks or twinning with orthorhombic symmetry and composition intermediate between protoenstatite and pigeonite in the system forsterite–diopside–silica. We have presented preliminary experimental results confirming the presence of the third low-Ca pyroxene (Longhi and Boudreau, 1979), which we will call "ortho-enstatite," and now report results of our completed investigation.

Our results are consistent with those of two other studies of which we were unaware until after the first draft of this paper was completed. Schwab and Jablonski (1973) reported coexisting iron-free orthopyroxene, forsterite, and melt at 1410°C, produced during differential thermal analysis of pigeonite with composition  $\text{Ca}_{0.2}\text{Mg}_{1.8}\text{Si}_2\text{O}_6$ . Foster and Lin (1975) reported, in abstract, results of melting experiments similar to ours. Some minor differences in temperature of some of the invariant points exist between the two studies, and Foster and Lin have not reported solid solution limits, but by and large the two studies confirm one another.

In what follows we will observe the following conventions for abbreviations: forsterite = Fo, protoenstatite = Pr, clinoenstatite = CEn, orthoenstatite = OEn, pigeonite = Pi, diopside = Di, tridymite = Tr, and cristobalite = Cr. All of the phases are solid solutions, so we will not use the "ss" subscript. Although clinoenstatite and pigeonite are apparently isostructural at room temperature, both with  $P2_1/c$  space group, we will distinguish between the two on the basis of crystallization history: clinoenstatite forms during cooling as an inversion product from protoenstatite ( $Pbcn$ ), whereas pigeonite inverts during cooling from low-Ca pyroxene ( $C2/c$ ) with diopside structure (Prewitt *et al.*, 1971). Because the inversion from protoenstatite to clinoenstatite involves a more severe disruption of structure and volume change than does the inversion from diopside to pigeonite, clinoenstatite contains abundant cracks and polysynthetic twinning, whereas pigeonite does not.

### Experimental methods

Initially, three bulk compositions (A, B, C, Table 1) in the system Fo–Di–SiO<sub>2</sub> were prepared by multiple grindings and fusions of reagent-grade oxide mixtures. After the glasses were homogeneous (except C, which retained a small amount of unmelted

silica), they were ground once more and devitrified at 1200°C for four days. Derivative compositions, D and E, were obtained by mixing devitrified A and B in a 4 to 1 ratio and devitrified B and C in a 4 to 3 ratio respectively. Derivative composition F was obtained by adding approximately 20 wt. percent MgSiO<sub>3</sub> as oxides to B and then fusing and grinding the mixture twice.

The devitrification produced sub-microscopic intergrowths of crystals. These materials were used in all experiments except as noted in Table 2. Qualitative energy-dispersive analysis with the finely focused beam of a JEOL JSM-35 scanning electron microscope showed distinct regions of high and low Ca. An X-ray diffractometer scan of mix A showed it to be a mixture of low-Ca clinopyroxene—presumably pigeonite—and diopside. Individual reflections were quite diffuse: peak widths at one-half peak maximum were 1.5 to 2 times the widths of peaks measured in diffractometer scans of the run products. An estimate of the position of the 220 reflection, referenced against Si metal, was made in order to measure the average composition of the low-Ca clinopyroxene from the determinative curve of Boyd and Schairer (1964, Fig. 4). The measured angle was 27.93°  $2\theta$ , which gives approximately 28 wt. percent diopside. Pyroxene with such a composition is undoubtedly metastable. Given the euhedral morphologies of 10 to 100  $\mu\text{m}$  crystals produced in the melting experiments as compared to the cryptocrystalline nature of the starting materials, it seems likely that the crystal growth process was one of dissolution and reprecipitation.

The devitrified starting materials were loaded into sections of 1/4" Pt tubing approximately 1 cm long, welded shut at the bottom and crimped at the top. Charges were suspended in a Deltec T-31 Super Kanthal furnace and were dropped directly into cold water at the end of each experiment. Temperature was measured with a 94Pt6Rh/70Pt30Rh thermocouple calibrated against the melting point of gold

Table 1. Nominal compositions of starting materials

Composition:	A	B	C	D	E	F
	wt % oxides					
SiO <sub>2</sub>	58.1	62.1	66.0	58.9	63.8	61.7
MgO <sup>2</sup>	30.5	26.5	21.7	29.7	24.4	28.8
CaO	11.4	11.4	12.3	11.4	11.8	9.5
	wt coordinates					
Fo	.390	.320	.225	.376	.278	.383
Di	.440	.440	.475	.340	.456	.367
SiO <sub>2</sub>	.170	.240	.300	.184	.266	.250

Table 2. Electron microprobe analyses in weight percent oxides of coexisting phases in the system forsterite–diopside–silica

RUN	TEMP (°C)	TIME (hrs)	PHASE	SiO <sub>2</sub>	MgO	CaO	Sum	No. of Points	H (CaO)	COMMENTS
Forsterite/Protoenstatite Boundary										
A-6	1445	89	L	60.0	27.5	12.4	99.9	4	1.3	probable OEn; Fo present single crystal analyzed
			Pr	60.1	39.1	0.63	99.8	4	0.7	
Protoenstatite/Orthoenstatite Boundary										
B-2	1435	48	L	61.5	24.6	13.0	99.1	4	0.9	held at 1391°C for 3 days
			Pr	59.8	39.4	0.71	99.9	4	0.2	d.c.
			OEn	58.7	37.8	1.87	98.4	3	0.7	d.c.
B-8	1435	66	L	61.7	25.0	12.7	99.4	4	0.7	OEn present
			Pr	59.7	38.8	0.67	99.2	3	0.6	d.c.
E-3	1419	70	L	62.9	22.9	13.3	99.1	4	0.5	Tr present
			Pr	59.0	38.6	0.76	98.4	3	1.4	d.c.
			OEn	59.2	38.4	1.45	99.0	5	0.8	d.c.
Forsterite/Orthoenstatite Boundary										
A-2	1435	48	L	58.5	26.2	13.9	98.6	4	0.8	held at 1391°C for 3 days
			Fo	43.5	57.7	0.50	101.7	4	1.9	d.c.
			OEn	59.8	39.2	1.61	100.6	4	2.1	d.c.
A-8	1435	66	L	57.8	26.3	13.9	98.0	4	1.1	Fo present
			OEn	60.2	38.4	1.59	100.2	4	1.6	d.c.
A-11	1421	96	L	58.9	25.3	14.5	98.7	4	1.3	Fo present
			OEn	59.8	38.1	1.73	99.6	4	1.4	d.c.
A-1	1414	103	L	58.7	24.9	14.9	98.5	4	1.0	d.c. 2.0-2.3 wt% CaO; d.c.
			Fo	42.7	55.9	0.54	99.1	2	2.9	
			OEn	59.5	38.4	2.09	100.0	5	3.0	
Orthoenstatite/Pigeonite Boundary										
B-13	1395	451	L	61.9	21.0	15.4	98.3	5	0.8	1.96-2.10 wt% CaO; 2 crystals analyzed d.c.
			OEn	59.5	38.0	2.01	99.5	10	2.0	
			Pi	59.4	37.2	3.03	99.6	10	1.3	
B-3	1387	96	L	62.8	21.5	15.8	100.1	4	0.8	Tr present
			OEn	60.4	37.8	2.24	100.5	4	1.6	d.c.
			Pi	58.9	37.0	3.46	99.4	9	2.7	3.2-3.8 wt% CaO; d.c.
Forsterite/Pigeonite Boundary										
A-4	1407	160	L	58.7	24.3	16.2	99.2	4	1.2	Fo present
			Pi	59.4	37.5	3.37	100.3	3	3.5	3.2-3.6 wt% CaO; d.c.
A-3	1387	96	L	57.3	23.5	17.7	98.5	4	0.7	d.c. 4.8-5.4 wt% CaO; d.c.
			Fo	43.5	56.5	0.61	100.6	2	0.5	
			Pi	59.2	35.5	5.11	99.8	3	3.4	
Pigeonite/Diopside Boundary										
D-3	1378	1155	Pi	58.8	34.8	6.06	99.7	13	4.2	5.46-7.68 wt% CaO; d.c.
			Di	56.8	25.4	17.7	99.9	10	3.4	16.7-18.1 wt% CaO; d.c. held at 1423°C for 7 hrs
D-4	1378	1155	L	60.3	21.1	17.6	99.0	5	2.0	5.78-6.38 wt% CaO; d.c. 17.1-18.5 wt% CaO; d.c.
			Pi	58.8	35.0	6.07	99.8	10	3.1	
			Di	56.9	25.6	18.0	100.5	10	3.7	
A-13	1378	1155	L	59.3	22.2	17.7	99.2	6	1.0	6.07-6.41 wt% CaO; d.c. 16.4-18.2 wt% CaO; d.c.
			Pi	59.2	34.9	6.22	100.3	6	2.2	
			Di	56.9	25.5	17.6	100.0	6	5.0	
A-5	1380	142	Pi	59.0	34.9	6.50	100.4	4	4.9	5.8 - 6.9 wt% CaO; d.c.
			Di	56.6	26.3	16.6	99.5	3	2.5	16.2-16.9 wt% CaO; d.c.

(1064°C) and the liquidus of diopside (1392°C). Calibrations were made before, during, and at the end of the study. The thermocouple showed no sign of deterioration during the first thousand hours of this study;

during the second thousand hours the thermocouple decalibrated approximately 5°C and was replaced. In each calibration the difference between the gold and diopside calibrations was no more than 3°C. Re-

Table 2. (continued)

RUN	TEMP (°C)	TIME (hrs)	PHASE	SiO <sub>2</sub>	MgO	CaO	Sum	No. of Points	H (CaO)	COMMENTS
Tridymite/Orthoenstatite Boundary										
B-14	1406	304	L	61.8	22.6	14.3	98.7	5	1.0	Tr present; held at 1479°C 2hrs d.c.
			OEn	60.0	38.2	1.67	99.9	15	1.7	
B-15	1406	304	L	61.6	22.3	14.5	98.7	9	1.7	Tr not observed d.c.
			OEn	59.9	38.3	1.74	99.9	15	1.7	
E-5	1406	304	L	62.2	22.0	14.3	98.5	5	0.9	Tr present d.c.
			OEn	59.8	38.4	1.70	99.9	15	1.9	
C-9	1400	143	L	63.1	22.0	14.5	99.6	4	1.0	Tr present d.c. d.c.
			OEn	59.3	38.0	1.74	99.0	4	1.1	
			OEn	60.1	37.7	2.51	100.3	4	1.3	
E-4	1395	451	L	61.6	21.2	15.1	97.9	5	0.6	Tr present d.c.
			OEn	59.8	38.3	1.96	100.1	10	1.1	
Tridymite/Pigeonite Boundary										
C-3	1387	96	L	61.8	20.8	15.7	98.3	4	1.6	possible OEn - optical 0.12-0.19 wt% CaO; d.c. 3.5 - 4.0 wt% CaO; d.c.
			Tr	98.7	0.06	0.16	98.9	2	3.5	
			Pi	59.6	36.8	3.73	100.1	5	3.3	
B-5	1380	142	L	63.5	20.5	16.4	100.4	4	1.1	Tr present d.c.
			Pi	59.4	36.1	4.23	99.7	6	1.5	
C-5	1380	142	L	61.6	20.1	16.5	98.2	4	1.6	Tr present d.c.
			Pi	59.5	35.8	4.98	100.3	4	1.1	
Protoenstatite Liquidus Field										
B-7	1455	50	L	62.3	26.0	12.1	100.4	4	0.7	0.58-0.68 wt% CaO; d.c.
			Pr	60.3	39.4	0.63	100.3	4	2.3	
B-6	1445	89	L	61.7	25.6	12.4	99.7	4	1.1	d.c.
			Pr	60.0	39.4	0.66	100.1	6	1.2	
Orthoenstatite Liquidus Field										
F-13	1416	96	L	62.0	23.3	13.6	98.9	4	0.7	d.c.
			OEn	60.0	38.3	1.49	99.8	4	0.8	
B-1	1414	103	L	61.4	23.0	14.0	98.4	4	0.4	1.7-1.9 wt% CaO; d.c.
			OEn	59.2	38.2	1.80	99.2	5	2.3	
B-9	1400	143	L	62.7	22.1	15.1	99.9	4	1.9	1.8-2.0 wt% CaO; d.c. d.c.
			OEn	59.9	37.9	1.89	99.7	5	2.4	
			OEn	59.8	37.3	2.71	99.8	4	1.0	

d.c. = each point located on a different crystal

ported temperatures are referenced to the diopside liquidus. Based upon the reproducibility of replicate experiments, we estimate the precision of our temperature control and measurement to be  $\pm 3^\circ\text{C}$ ; absolute accuracy is  $\pm 5^\circ\text{C}$ .

Run products were crushed and examined under oils; chips were set in epoxy, polished, and analyzed with an ARL-EMX-SM electron microprobe. Natural enstatite (Si, Mg) and diopside (Ca) served as standards for olivine, pyroxene, and tridymite; synthetic glasses (Dalheim, 1977) served as standards for the glasses. The various phases were readily distinguished by their distinct fluorescence colors under the electron beam. Typically, counts were taken on four or more distinct spots on each phase (separate

crystals when available) in each run and the homogeneity index, H (Boyd *et al.*, 1967), was calculated for each element. Glass, forsterite, and protoenstatite were the most homogeneous phases ( $H \leq 1.5$ ). As noted in the tables below, orthoenstatite, pigeonite, and diopside were more heterogeneous, though their compositional ranges remained distinctive.

Despite the rapid quenching of the run products, many of the olivine and pyroxene crystals in the near-liquidus runs have collars of quench crystals up to 10  $\mu\text{m}$  wide that are readily discernable in both transmitted and reflected light. Multiple spot analyses of the glasses shows no detectable differences in composition throughout the charges regardless of the presence or absence of crystals. Apparently quench

growth had only very local effects on glass composition and presented no problems as long as the tiny quench areas were avoided.

## Results

### Liquidus fields

Compositions of coexisting crystals and liquid are listed in Table 2. Revised liquidus boundaries and data points in the Fo–Di–SiO<sub>2</sub> system are shown in Figure 1 along with data points from Kushiro (1972) and Boyd and Schairer (1964). Apart from the liquidus field of orthoenstatite, there is general agreement among the various data sets. Our data show the protoenstatite/orthoenstatite liquidus boundary to be at somewhat lower diopside content than Kushiro's protoenstatite/"pigeonite" boundary. This discrepancy is due to a minor error by Kushiro in assigning

a temperature to the Fo + Pr + OEn("Pi") + L peritectic, as we shall discuss below. We have also observed some other discrepancies between our liquidus data and those of Kushiro. For example, two of our runs at 1435°C along the Fo + OEn liquidus curve (Figs. 1 and 2, Table 2) have a slightly higher diopside content than Kushiro's reported 1430°C run. Our data also show the pigeonite/diopside liquidus boundary lying at higher diopside content than determined by Kushiro. At some temperatures, however, there is good agreement, for example 1387° (ours) vs. 1385°C (Kushiro's). We suspect that a difference in microprobe standards may have contributed to these discrepancies.

The compositions of the one-atmosphere invariant points, Pr + OEn + Tr + L (1419±5°C) and OEn + Pi + Tr + L (1387±5°C), have been determined directly by microprobe analysis of quenched liquids

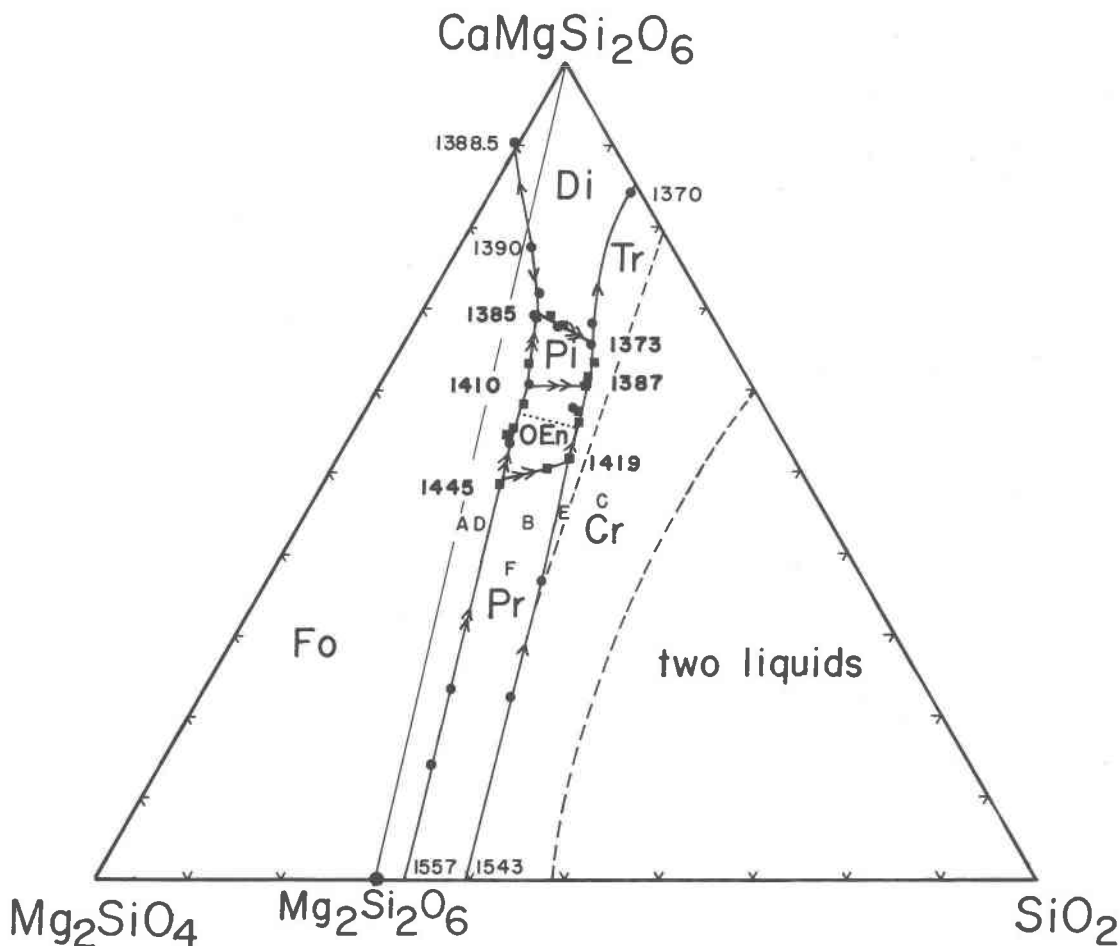


Fig. 1. Liquidus boundaries in the system forsterite–diopside–silica at one atmosphere (weight proportions). Symbols represent liquid compositions saturated with two or more crystalline phases: circles—Kushiro (1972), squares—this study. Dotted line is "Pr/Pi" boundary from Kushiro (1972, Fig. 1). Single arrows indicate cotectic curves; double arrows indicate reaction curves.

(Fig. 1 and Table 2). Though we have not been able to locate and analyze orthoenstatite with the microprobe in polished chips of the 1445°C run (A-6), optical examination of the crushed products suggests its presence along with Fo and Pr. Therefore, we tentatively set the Pr + OEn + Fo + L invariant point at  $1445 \pm 5^\circ\text{C}$ . The previously unrecognized phase boundary, that between orthoenstatite and pigeonite, has been located along the forsterite liquidus by bracketing runs. The slope of the OEn/Pi boundary curve, though not precisely determined, is sufficiently constrained so that a tangent to the curve will intersect the pyroxene join at diopside contents well beyond the range of OEn and Pi solid solutions;

hence, OEn will react with liquid along this curve to form Pi. It follows from similar considerations that the Pr/OEn liquidus boundary is also a reaction curve and that the Pr + OEn + Fo + L, Pr + OEn + Tr + L, OEn + Pi + Fo + L, and OEn + Pi + Tr + L invariant points are all peritectics involving the consumption of the pyroxene phase lower in Ca.

Liquid compositions along the forsterite/pyroxene liquidus boundary are shown projected from  $\text{Mg}_2\text{SiO}_4$  onto the  $\text{Mg}_2\text{Si}_2\text{O}_6$ - $\text{CaMgSi}_2\text{O}_6$  join in Figure 2 as solid lines. The liquidus of compositions along the  $\text{Mg}_2\text{Si}_2\text{O}_6$ - $\text{CaMgSi}_2\text{O}_6$  join is shown as a dashed curve. The temperature maximum along the forsterite + diopside cotectic is taken from Kushiro

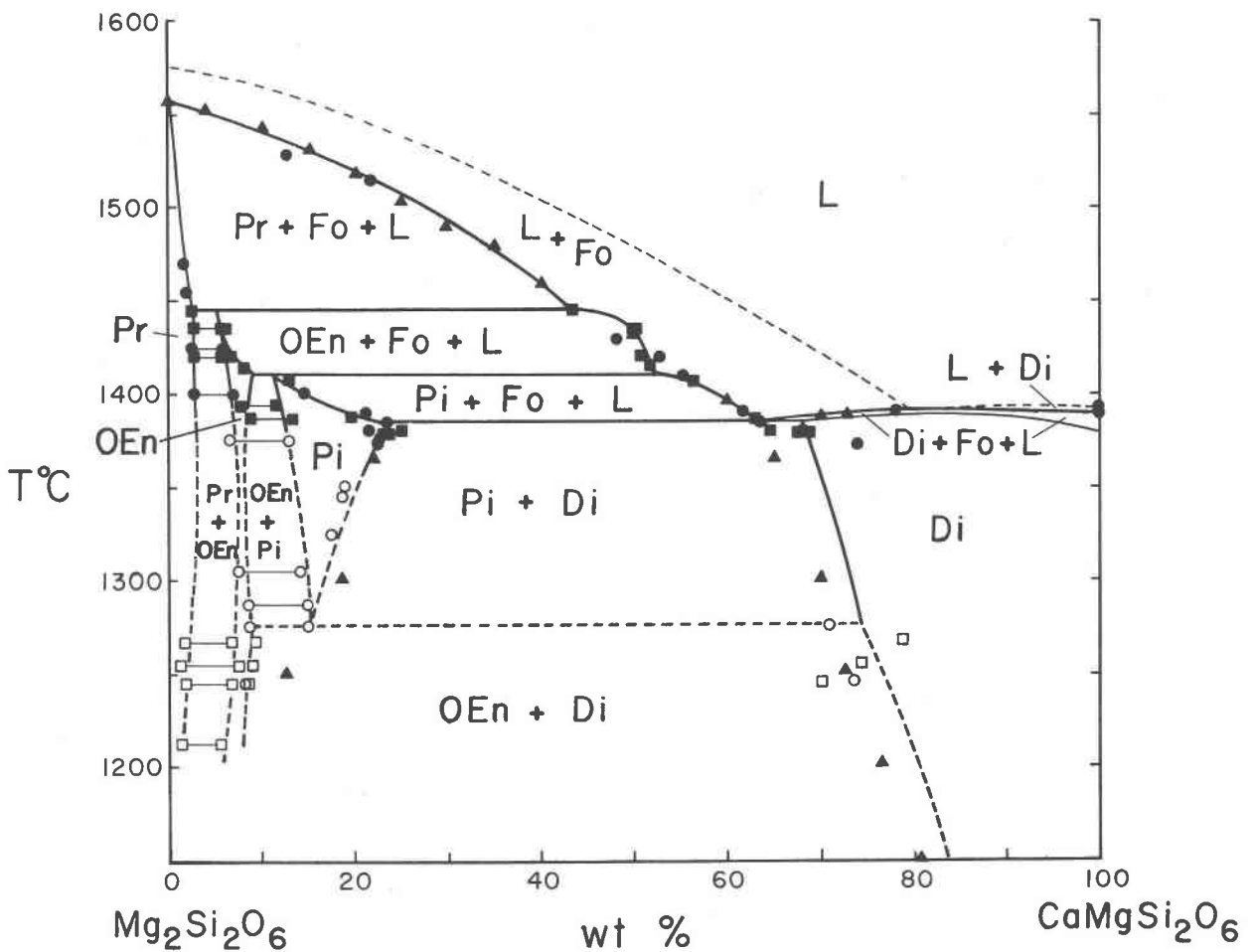


Fig. 2. Solid solution in the melting interval of a portion of the system forsterite-diopside-anorthite-silica projected onto the  $\text{Mg}_2\text{Si}_2\text{O}_6$ - $\text{CaMgSi}_2\text{O}_6$  join. Solid symbols are Al-free compositions in the system Fo-Di-SiO<sub>2</sub>; open symbols are aluminous compositions projected from  $\text{CaAl}_2\text{Si}_2\text{O}_6$ . Liquid compositions are projected from  $\text{MgSiO}_4$ . Heavy solid lines are phase boundaries in the system Fo-Di-SiO<sub>2</sub>; upper dashed line is the liquidus of the  $\text{Mg}_2\text{Si}_2\text{O}_6$ - $\text{CaMgSi}_2\text{O}_6$  join; subsolidus dashed lines are phase boundaries projected from the Fo-Di-An-SiO<sub>2</sub> system. Light solid lines are tie lines between coexisting low-Ca pyroxene; lines to diopside are not shown. Symbols: solid circles—Kushiro (1972); solid triangles—Boyd and Schairer (1964); solid squares—this study; open circles—Yang (1973); open squares—Longhi (1978).

and lies approximately where the Fo + Di cotectic crosses the pyroxene join. Due to the projection, compositions which lie along the join and crystallize Fo first will follow a path of nearly constant apparent diopside content in the temperature interval between Fo and pyroxene crystallization (actually the projected diopside content of the crystallizing liquid will decrease slightly because of the small Ca content of forsterite).

#### *Solid solution in the melting interval*

Temperature-composition relations of pyroxene solid solutions coexisting with liquid are shown in Figure 2. Microprobe analyses show highly restricted compositional ranges of protoenstatite (<3 wt. percent Di) and orthoenstatite (6–9 wt. percent Di), whereas pigeonite and diopside have more extensive ranges. Data from this study and from Kushiro are solid symbols and define binary pyroxene phase relations. Only the compositions of pyroxenes coexisting with forsterite plus liquid define the apparent solidus. However, because of the binary nature of the pyroxene solid solution in this system—diopside is a slight exception (Kushiro, 1972)—two coexisting pyroxenes define a two-phase field regardless of the presence of forsterite or other phases. Thus coexisting pyroxenes along the proto/orthoenstatite, orthoenstatite/pigeonite, and pigeonite/diopside liquidus boundaries (Fig. 1) may be used to define portions of the “sub-solidus” two-phase fields. Kushiro assigned a temperature of 1425°C for the reaction  $Pi$  (actually OEn)  $\rightleftharpoons Pr + Fo + L$  on the basis of coexisting pyroxenes (Kushiro, Table 2). Since Kushiro made no mention of forsterite in this run, we suspect that the liquid composition in this run lies off the forsterite saturation surface along the proto/orthoenstatite liquidus boundary. If so, then the peritectic involving forsterite must lie at a higher temperature as indicated in Figure 2 (1445±5°C).

Typically, in runs of 100–200 hours duration different crystals of orthoenstatite or clinopyroxene have a compositional spread somewhat beyond the precision of the microprobe: values of the homogeneity index,  $H$ , range from 2.0 to 3.5. Much longer run times are required to produce pyroxenes as homogeneous as the glasses. However, the uncertainty in the pyroxene analyses is not significant with respect to the topology and extent of the fields in Figure 2—the size of the symbols represents the approximate uncertainty in the compositions. One set of runs, B-9 and C-9 at 1400°C for 143 hours, produced two distinct sets of orthoenstatite compositions (Table 2). The

OEn lower in Ca also fluoresced a brighter blue color under the electron beam and so was readily distinguishable. We suspected that the OEn higher in Ca was metastable, having formed in reaction with pigeonite in the starting mixes as the charge heated up. This suspicion was apparently borne out by the results of longer runs at 1406°C for 304 hours (B-14, B-15, E-5) and at 1395°C for 451 hours (B-13, E-4) in which only one orthoenstatite phase was detected. The high-Ca OEn in B-9 and C-9 have compositions intermediate between the compositions of coexisting  $Pi$  and OEn in run B-13, whereas the low-Ca OEn in B-9 and C-9 have compositions similar to the OEn in runs B-13, E-4, B-14, B-15, and E-5. The apparent sluggishness of reactions involving iron-free pyroxenes at these high temperatures in the presence of 60–70 percent melt is rather surprising.

Month-long experiments at 1378°C (D-3, D-4, A-13, Table 2) with various starting materials give compositions of coexisting pigeonite and diopside quite similar to one another, but notably different from those of week-long experiments at 1380°C. The composition gap between pigeonite and diopside is 4–5 wt. percent Di wider in the 1378° runs than in the 1380° run (Table 2). This disparity suggests that the 1380° run did not equilibrate as extensively as the 1378° runs. Our results at 1378° may also be compared with those of Boyd and Schairer (1964) and Kushiro (1972) in Figure 2. There is closer agreement among the data sets on the pigeonite limb of the solvus than on the diopside limb, where data points of Boyd and Schairer (1964) are lower than ours and Kushiro's by 4–7 wt. percent Di. Some of this disparity is probably due to inaccuracies in the X-ray determinative curves employed by Boyd and Schairer (1964). Given (a) the convergence of pyroxene analyses in our 1378°C runs with different starting materials (D-3 started off as glass + forsterite + orthoenstatite, whereas D-4 and A-13 started off as cryptocrystalline clinopyroxene intergrowths), (b) the longer run times in our experiments (4 weeks as opposed to 3 to 14 days), and (c) the more extensive analyses, we believe our data to represent the closest approach to equilibrium yet reached in the near-sub-solidus portion of the  $Mg_2Si_2O_6$ – $CaMgSi_2O_6$  system and have drawn the pigeonite/diopside solvus in Figures 2 and 3 accordingly. However, strict reversals of the solvi compositions still remain to be done.

Open symbols in Figure 2 are pyroxene compositions from Yang (1973) and Longhi (1978 and unpublished) in the system Fo–Di–An– $SiO_2$ , which are projected from  $CaAl_2SiO_6$  and define certain ternary

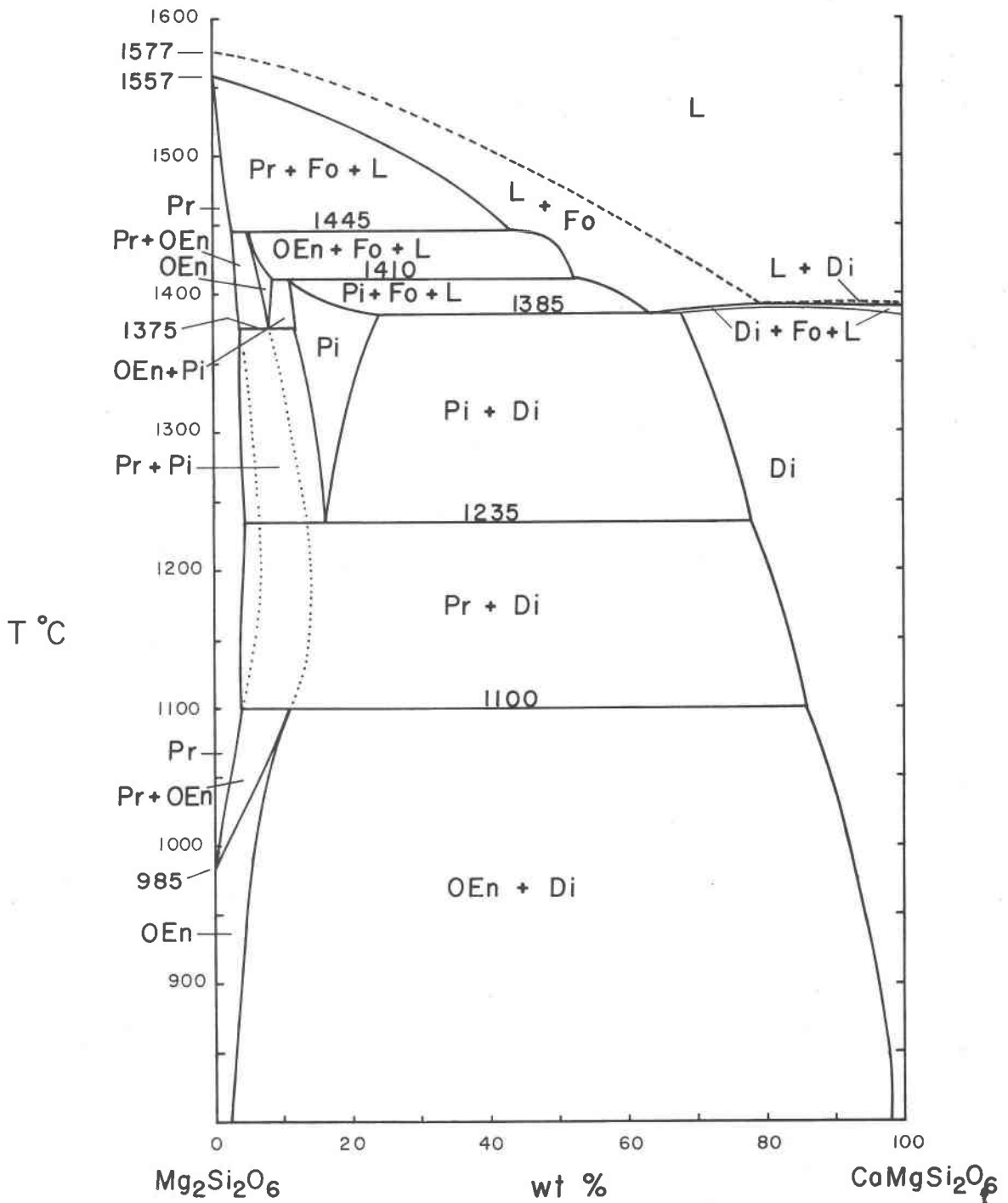


Fig. 3. Subsolidus phase equilibria and solid solution in the system  $\text{Mg}_2\text{Si}_2\text{O}_6$ - $\text{CaMgSi}_2\text{O}_6$ . Dotted line is inferred metastable two-phase field of protoenstatite and orthoenstatite.

phase relations. Because of the higher variance, these data do not define unique binary phase relations and thus appear to fit awkwardly on the diagram. The data are presented, however, to illustrate (a) the sta-

bility of iron-free orthoenstatite at temperatures where it was previously thought to be unstable, and (b) the limited ranges of diopside component in Pr and OEn. The subsolidus phase relations in the

aluminum-free  $\text{Mg}_2\text{Si}_2\text{O}_6$ - $\text{CaMgSi}_2\text{O}_6$  system are not necessarily analogous to those indicated in Figure 2 by the dashed lines.

#### *The subsolidus region*

After much intensive study (Atlas, 1952; Boyd and Schairer, 1964; Warner and Luth, 1974) the subsolidus phase relations in the system  $\text{Mg}_2\text{Si}_2\text{O}_6$ - $\text{CaMgSi}_2\text{O}_6$  still defy precise representation, because of sluggish kinetics and confusing X-ray diffraction results. Boyd and Schairer noted that run times of several days to weeks are insufficient to bring enstatite-rich compositions to equilibrium below 1250°C in the absence of water or a flux. Warner and Luth have pointed out that X-ray powder patterns for iron-free clinoenstatite and pigeonite are virtually indistinguishable except for a discontinuity in cell volumes as diopside content increases. For this reason pigeonite was overlooked (Atlas, 1952; Boyd and Schairer, 1964) and much of what is actually pigeonite was identified as clinoenstatite. In the melting interval where crystals may grow up to 100  $\mu\text{m}$  long, distinguishing the two phases is a relatively simple matter by optical examination: if clinoenstatite has formed by inversion from protoenstatite, clinoenstatite will be cracked and polysynthetically twinned whereas pigeonite crystals will be smooth-appearing with rare twinning. Unfortunately, this distinction was not made until the work of Yang and Foster (1972) and Kushiro (1972).

In view of these circumstances, it is not surprising that the extent of the pigeonite field remains uncertain in the subsolidus region of the  $\text{Mg}_2\text{Si}_2\text{O}_6$ - $\text{CaMgSi}_2\text{O}_6$  system. Yang (1973) has shown that the pigeonite field shrinks and finally pinches out with decreasing temperature in the  $\text{Fo-Di-An-SiO}_2$  system. He reversed the reaction  $\text{Pi} \rightleftharpoons \text{Pr} + \text{Di} + \text{L}$  at 1276°C. Since his "protoenstatite" was free of cracks and the data of Longhi (1978) shown in Figure 2 suggest a probable orthoenstatite stability field at 1276°C, the reaction was actually  $\text{Pi} \rightleftharpoons \text{OEn} + \text{Di} + \text{L}$ . Regardless of the identity of the orthorhombic pyroxene, however, the reaction is univariant in the aluminous system at one atmosphere, and so persists over a range of temperature. In the  $\text{Mg}_2\text{Si}_2\text{O}_6$ - $\text{CaMgSi}_2\text{O}_6$  system Boyd and Schairer (1964) have reported clinoenstatite with 12.5 wt. percent diopside in solid solution as low as 1250°C at 1 atmosphere; this phase is almost certainly pigeonite. Atlas (1952) proposed the reaction  $\text{CEn} \rightleftharpoons \text{Pr} + \text{Di}$  at 1235°C on the basis of a small shift in the observed diopside content in clinoenstatite between 1235°C (17 mole

percent) and 1200°C (12 mole percent) and on the basis of "decrepitation" of experimental charges within the low-Ca pyroxene/diopside two-phase field below 1250°C (he observed that the inversion of protoenstatite to clinoenstatite caused crystalline charges to become friable). Again, Atlas' "undecreptated clinoenstatite" is probably pigeonite and the reaction  $\text{Pi} \rightleftharpoons \text{Pr} + \text{Di}$  is given at 1235°C in Figure 3. The uncertainty of this reaction is large because of the unknown solution effects of the fluxes used by Atlas on the relative stabilities of the pyroxene phases. The data apparently indicate, however, that Al diminishes the thermal stability of pigeonite.

Recognition of a field of orthoenstatite in the melting interval creates additional complexities. Previously, it was believed that the upper temperature stability limit of orthoenstatite solid solution, free of Al and Fe, was approximately 1100°C (Boyd and Schairer, 1964), and that orthoenstatite broke down according to the reaction  $\text{OEn} \rightleftharpoons \text{Pr} + \text{Di}$  as shown in Figure 3. Also, careful examination of enstatite-rich run products at 1365°C (Boyd and Schairer, 1964) and at 1350° (Warner and Luth, 1974) failed to reveal any orthoenstatite. Boyd and Schairer did, however, report orthoenstatite ("rhombic enstatite") at 1395°C, which they interpreted as a quench product "... inasmuch as the rhombic form has been proved to be unstable at these temperatures." We, however, have observed orthoenstatite in the temperature interval 1387°-1435°C coexisting with pigeonite, protoenstatite, forsterite and liquid. Runs A-2 and B-2 were equilibrated within the pigeonite field for a day before raising the temperature to 1435°C: pigeonite converted entirely to orthoenstatite and so there is no doubt that orthoenstatite is a stable phase at these temperatures. The various data may be reconciled by the reaction  $\text{OEn} \rightleftharpoons \text{Pi} + \text{Pr}$  which is shown to terminate the high-temperature orthoenstatite field at  $1375 \pm 10^\circ\text{C}$  in Figure 3. The result is a highly complex phase diagram with two distinct fields of orthoenstatite and orthoenstatite + protoenstatite separated by a 275°C interval. Additional work is needed to constrain the solvi more precisely. Indeed, we have drawn the pigeonite limb of the pigeonite/diopside solvus on the basis of our 1378°C runs and Boyd and Schairer's 1365° and 1300° runs—inferring the 1200° Boyd and Schairer run to contain clinoenstatite plus pigeonite. Thus the pigeonite limb of the solvus in Figure 3 is drawn to be about 4 wt. percent richer in diopside component at 1250°C than Figure 1 of Boyd and Schairer. We have also drawn the protoenstatite limb of the solvus

to be less than 4 wt. percent diopside at 1100°C, in contrast to the nearly 10 percent indicated by Atlas (1952), in order to be consistent with the protoenstatite analyses of Longhi (1978) and to satisfy topological constraints. At present we believe the topology of Figure 3 to be correct with respect to the existence of two distinct fields of orthoenstatite. Future work may well necessitate revision of the phase boundaries in the temperature range 1000°–1200°C, though, since these boundaries are rather poorly constrained.

### Discussion

The addition of an orthoenstatite liquidus field to the system Fo–Di–SiO<sub>2</sub> is significant because now all four common pyroxene phases found in basaltic rocks are together in a single system that can be used as an intuitive guide to pyroxene crystallization. Features of general interest are: (1) the incongruent melting of all three low-Ca pyroxene phases to forsterite + liquid; (2) the progression from protoenstatite to orthoenstatite to pigeonite liquidus fields with increasing diopside component in the melt; and (3) the reaction relationships between protoenstatite and orthoenstatite and between orthoenstatite and pigeonite along their respective liquidus boundaries. Unfortunately, the natural system displays far more complexity than can be represented in a single diagram, due to the interplay of addition components such as Al<sub>2</sub>O<sub>3</sub>, FeO, and alkalis, so that crystallization sequences not suggested here, such as augite → orthopyroxene, are encountered in nature. Longhi and Boudreau (1979) have illustrated some of the effects of these components in synthetic analogues of natural liquids, such as the shrinking of the pigeonite liquidus field with increasing anorthite component in the melt or the expansion of the pigeonite field at the expense of orthoenstatite with increasing Fe/Mg. Additional work is in progress.

The unusual topology of the subsolidus fields in Figure 3 suggests a bow-like shape for the metastable extension of the protoenstatite + orthoenstatite two-phase fields. Intersection of the diopside and pigeonite fields with the two-phase field leaves the center part of the bow metastable and results in two distinct fields of orthoenstatite separated by a 275°C temperature interval. The bow-like shape for a two-phase field with curvature normal to the temperature axis is not common in silicate systems, but is readily found in alloys, e.g. Fe–Si (Smithells, 1962, p. 683). It is possible to produce such a two-phase field between phases A and B, if there are two temperatures at

which  $G_A^\circ = G_B^\circ$ , where  $G^\circ$  denotes the free energy of the pure phase. For Mg<sub>2</sub>Si<sub>2</sub>O<sub>6</sub>, the lower temperature would be 985°C, while the higher temperature would be higher than 1550°C and obscured by melting. Alternatively, the bow shape might be produced by the intersection of two distinct two-phase fields such as A + B and A + B', where B and B' are polymorphs. This would require yet another distinct orthorhombic pyroxene structure at high temperature with a first-order transformation between the high- and low-temperature forms somewhere between 1375° and 1100°C. However, diffractometer scans of orthoenstatite from several runs and the powder pattern of Atlas (1952) for enstatite synthesized at 950°C are quite similar. Also we have obtained a least-squares refinement of the unit-cell dimensions of orthoenstatite from run F-13 (1416°C) with the program of Appleman and Evans (1973):  $a = 18.274(4)$ ,  $b = 8.836(2)$ ,  $c = 5.206(2)\text{\AA}$ , and  $V = 840.6(3)\text{\AA}^3$  (scan speed 0.4° 2 $\theta$ /min, 0.04° 2 $\theta$  tolerance, 19 of 21 lines successful). These cell dimensions are comparable to those reported by Warner and Luth (1974). Likewise, the experimental data of Yang (1973) and Longhi (1978) suggest a single continuous field of aluminous orthoenstatite between 1200° and 1375°C; and the data of Warner (1975) suggest a single orthoenstatite field up to 1300°C at a pressure of 2 kbar. Thus it seems likely that another Mg<sub>2</sub>Si<sub>2</sub>O<sub>6</sub> polymorph is not required to explain the observed equilibria: the bow-like shape of the two-phase field is the result of the intersection of the  $G^\circ$  curves of protoenstatite and orthoenstatite at two temperatures. Single-crystal X-ray diffraction work remains to be done to confirm this hypothesis.

### Acknowledgments

We thank D. F. Weill for his support of this investigation, Jack M. Rice for discussing phase diagram topologies with us, and D. H. Lindsley for a helpful review. This research was supported by NASA grant NGL-38-003-022.

### References

- Appleman, D. E. and H. T. Evans, Jr. (1973) Job 9214: Indexing and least squares refinement of powder diffraction data. *Nat. Tech. Inf. Serv.*, U.S. Dept. Commerce, Springfield, Virginia, Document PB-216 188.
- Atlas, L. (1952) The polymorphism of MgSiO<sub>3</sub> and solid state equilibria in the system MgSiO<sub>3</sub>–CaMgSi<sub>2</sub>O<sub>6</sub>. *J. Geol.*, 60, 125–147.
- Bowen, N. L. (1914) The ternary system diopside–forsterite–silica. *Am. J. Sci.*, 38, 207–264.
- Boyd, F. R. and J. F. Schairer (1964) The system MgSiO<sub>3</sub>–CaMgSi<sub>2</sub>O<sub>6</sub>. *J. Petrol.*, 6, 275–309.
- , L. Finger and F. Chayes (1967) Computer reduction of

- electron microprobe data. *Carnegie Inst. Wash. Year Book*, 67, 210-215.
- Dalheim, P. A. (1977) *Calculation of Empirical Coefficients in Multicomponent Oxide Systems for the Reduction of Electron Microprobe Data*. M.S. Thesis, University of Oregon, Eugene, Oregon.
- Foster, W. R. and H. C. Lin (1975) New data on the forsterite-diopside-silica system (abstr.). *Trans. Am. Geophys. Union*, 56, 470.
- Kushiro, I. (1972) Determination of liquidus relations in synthetic silicate systems with electron probe analysis: the system forsterite-diopside-silica at 1 atmosphere. *Am. Mineral.*, 57, 1260-1271.
- Longhi, J. (1978) Pyroxene stability and the composition of the lunar magma ocean. *Proc. Lunar Planet. Sci. Conf.*, 9th, 285-306.
- and A. E. Boudreau (1979) Pyroxene liquidus fields in basaltic liquids at low pressure (abstr.). *Lunar and Planetary Science X*, 739-741.
- Prewitt, C. T., G. E. Brown and J. J. Papike (1971) Apollo 12 clinopyroxenes: high temperature X-ray diffraction studies. *Proc. Lunar Sci. Conf.*, 2nd, 59-68.
- Schwab, R. G. and K. H. Jablonski (1973) Der Polymorphismus der Pigeonite. *Fortschr. Mineral.*, 50, 223-263.
- Smith, J. V. (1969) Crystal structure and stability of the  $MgSiO_3$  polymorphs: physical properties and phase relations of Mg,Fe pyroxenes. *Mineral. Soc. Am. Spec. Pap.*, 2, 3-29.
- Smithells, C. J. (1962) *Metals Reference Book, Vol. 1*. Butterworths, London.
- Warner, R. D. (1971) *Experimental Investigations in the System CaO-MgO-SiO<sub>2</sub>-H<sub>2</sub>O*. Ph.D Thesis, Stanford University, Stanford, California.
- (1975) New experimental data for the system CaO-MgO-SiO<sub>2</sub>-H<sub>2</sub>O and a synthesis of inferred phase relations. *Geochim. Cosmochim. Acta*, 39, 1413-1421.
- and W. C. Luth (1974) The diopside-orthoenstatite two-phase region in the system  $CaMgSi_2O_6$ - $Mg_2Si_2O_6$ . *Am. Mineral.*, 59, 98-109.
- Yang, H. (1973) Crystallization of iron-free pigeonite in the system anorthite-diopside-enstatite-silica at atmospheric pressure. *Am. J. Sci.*, 273, 488-497.
- and W. R. Foster (1972) Stability of iron-free pigeonite at atmospheric pressure. *Am. Mineral.*, 57, 1232-1241.

*Manuscript received, June 11, 1979;*  
*accepted for publication, December 27, 1979.*